JOURNAL OF MATERIALS SCIENCE 32 (1997) 2013–2020

Characterization of functionally gradient epoxy/carbon fibre composite prepared under centrifugal force

N. J. LEE, J. JANG
Department of Chemical Technology, Seoul National University, San 56-1, Shinlimdong, Kwanakku, Seoul, Korea

M. PARK, C. R. CHOE*
Polymer Composite Laboratory, Korea Institute of Science and Technology, P.O. Box 131, Cheongryang, Seoul, Korea

Centrifugal force was employed in order to induce a spatial gradient of fibre distribution in the epoxy/carbon fibre system. The gradient structure of the epoxy/carbon fibre composite can be controlled by varying the rotation time and the material parameters, such as fibre length, fibre content and matrix viscosity. The spatial gradient distribution of carbon fibres in an epoxy matrix was achieved by the combined mechanism of packing and settling. The mechanical properties of the functionally gradient epoxy/carbon fibre composite were also investigated. At the same content of carbon fibre, the flexural strength of the functionally gradient composite was higher than that of conventional isotropic composite.

1. Introduction

Recently, new material concepts have been presented to induce various material properties. One of those concepts is related to functionally gradient material (FGM), which has continuous spatial distribution of two or more different components, with high performances such as effective thermal stress relaxation, adhesive property, and so on. The compositional gradient is introduced to improve the property of isotropic materials with the same composition along the thickness of the materials. This new material concept was first proposed in association with the development of super heat-resistant material for spaceplanes [1–3].

Fig. 1 represents a typical example of FGM. This material exhibits high thermal conductivity and mechanical strength at the metal surface and high thermal resistance at the ceramic surface. The gradient composition at the interface can effectively relax thermal stress concentration which may occur between two different materials [1, 2]. Niino and Maeda coated the SiC/C functionally gradient material on graphite substrate and tested the thermal fatigue property. As a result, they showed that the FGM had better thermal resistance and thermal fatigue property [2]. It was reported that the flexural modulus and strength of functionally gradient nylon 6/CF composite were higher than those of an isotropic nylon 6/CF composite [4]. Fukui *et al.* [5] performed a ring crushing test of corundum/plaster model composite prepared by centrifugal casting. They showed that the maximum load and the strain at break of the composite increased as the gradient of the composition became higher. Tsunekawa *et al.* [6] reported that when more alumina fibres were present in the outer layer, the bending strength of the aluminium/alumina fibre composite had a higher value than that of isotropic composite.

In addition to the improved thermal stress relaxation and adhesive property, the applications of FGMs have been expanded to other fields such as sensor technology, optics, electronics, magnetics, and so on [3, 7, 8]. The FGM concept has also been changed from the idea of materials with compositional gradient in space to that with functions varying in space and with time [7, 9, 10]. Most research activities are being performed to develop polymer composite materials that possess excellent environmental resistance and mechanical properties [11].

As a first step to exploit the FGM concept for a polymer composite system, centrifugal force was employed to give a compositional gradient of fibrous filler in a polymer matrix. The effects of gradient distribution on the flexural properties of the functionally gradient epoxy/carbon fibre composites were also discussed.

*Author to whom all correspondence should be addressed.

0022–2461

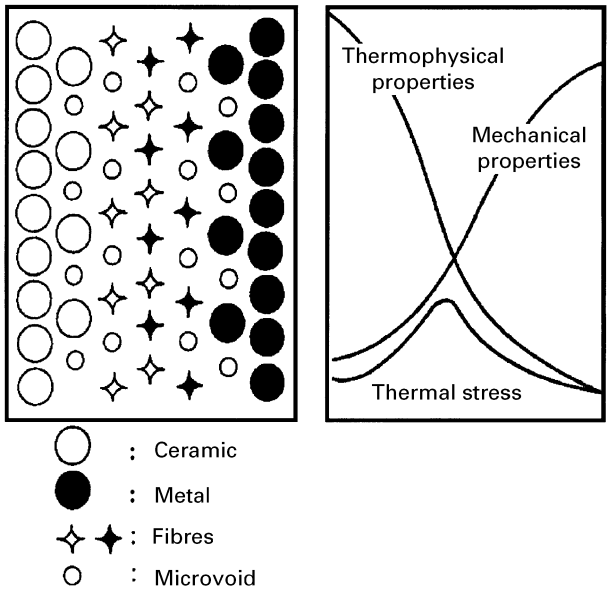

Figure 1 A typical example of a functionally gradient material [1].

TABLE I Milled carbon fibres used in this study

Code	Number average length, L_n (μm)	Weight average length, L_w (μm)	Poly dispersity (L_w/L_n)
CF-S	72	94	1.31
CF-M	116	160	1.38
CF-L	156	220	1.41

2. Experimental procedure

2.1. Materials

The carbon fibres (CF) used in this study (TZ-307, Taekwang Co. Korea, density 1.8 g cm^{-3}) were ball-milled to improve dispersion in the epoxy. They were classified by sieving into three species, according to their length. The average lengths of CFs were measured by a semi-automatic method with a digitizing tablet and computer, and the results are shown in Table I.

Bi-functional epoxy resin (DGEBA, YD-128, Kukdo Chemical Co., Korea) was used as a matrix resin. Diethylenetriamine (DETA) (Junsei Chemical Co., Japan) was used as a curing agent and 11 p.h.r. was mixed with YD-128. The density of the epoxy resin cured with 11 p.h.r. DETA was 1.19 g cm^{-3} at 23 °C.

2.2. Specimen preparation

After the CF/epoxy/DETA mixture was poured into a cylindrical glass test tube (diameter 18 mm), the test tube was rotated (Fig. 2). The rounded shape of the test tube was flattened beforehand to eliminate the converging part of the tube. A centrifuging machine HA-50 (Han Il Co., Korea) was used to impose the centrifugal force on the mixture for predetermined time periods, which were all within the gel time of the present epoxy system. The centrifugal force at 1000 r.p.m. was about 170 times the gravitational force.

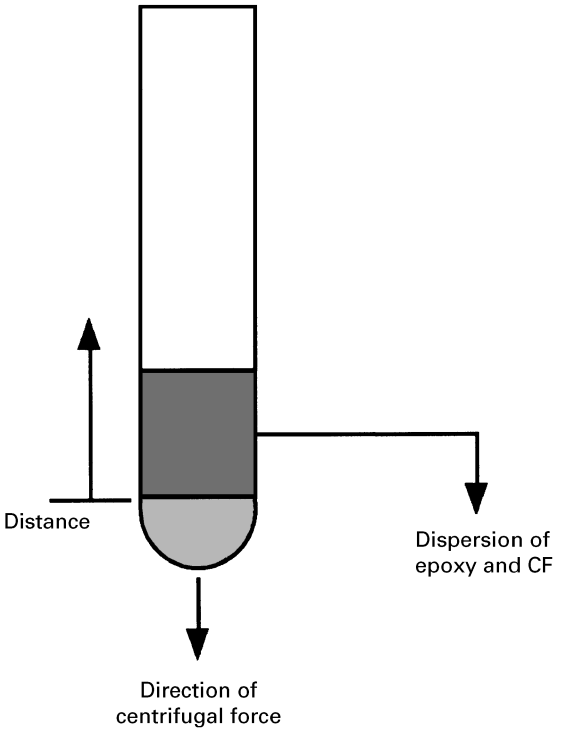

Figure 2 Schematic illustration of specimen preparation for density measurement.

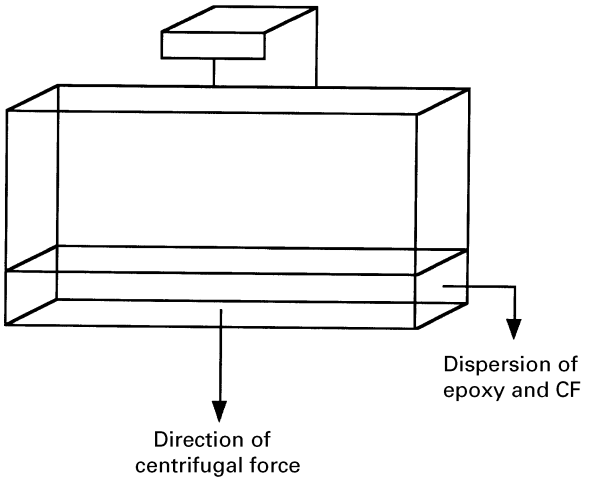

Figure 3 Schematic illustration of preparation of the bar-shaped specimen for the flexural property test.

The mixture in the test tube was cured at an ambient temperature for 24 h and post-cured at 100 °C for 2 h. The flexural property of the functionally gradient epoxy/CF composite was estimated using a bar-shaped specimen prepared using the mould shown in Fig. 3. The mixture in both the test tube and the bar-shaped mould experience the same centrifugal force because the radii of rotation were adjusted to be identical.

The mechanical properties of the isotropic epoxy/CF composite were measured with different contents of CF. Dog-bone shaped specimens were prepared to test the tensile property of epoxy/CF

composite with constant CF distribution. In addition, specimens for the compression test were also prepared.

2.3. Measurement

The density of the specimen was measured using a density gradient column (ASTM D-1505). The specimen was cut into thin sections perpendicular to the direction of centrifugal force. The cross-sections of the specimen, polished with fine alumina powder, were observed with videomicroscope (Scalar Co.).

Volume resistivities of the specimen were measured to verify indirectly the concentration and the orientation of CF inside the epoxy matrix. In order to make CF more conductive, gold-coating was performed with gold sputter S150B (Edwards, UK). Gold coating and mixing of CF on aluminium foil were performed several times to obtain an homogeneous coating. The specimen was cut into thin sections perpendicular to the direction of centrifugal force. Silver paste was used for good contact and connection with the copper line. The resistivity of the specimen was calculated from

$$\rho = R\frac{A}{t} \tag{1}$$

where R is the resistance of the sample (Ω), A is the cross-section area (cm^2) and t is the thickness (cm) of the sample.

A Universal testing machine (Instron 4201) was used to measure the mechanical properties of the epoxy/CF composite. A three-point bending test was performed to measure the flexural property. The support span was 5 cm, and the crosshead speed was 1 mm min^{-1}. The crosshead speed of the tensile test of the dog-bone type specimen was 10 mm min^{-1} and the grip distance was 35 mm. The compressive test specimen dimensions were 5 mm × 5 mm × 10 mm and the crosshead speed was 0.5 mm min^{-1}.

3. Results and discussion

3.1. Effect of centrifugal force

3.1.1. Effect of rotation time

The application of centrifugal force controlled by the speed and radius of rotation, would cause CFs in an epoxy/CF dispersion to move towards the applied force direction. For dispersions in which the volume fraction of filler ranges from 0.03–0.10, fillers are known to settle down according to the following equation, which simply introduces the correction factor, K_{crowd}, to Stoke's equation [12]

$$v = \frac{(\rho_f - \rho_m)\, g d_f^2}{18\eta} K_{crowd} \tag{2}$$

where v is the terminal velocity of the filler and ρ_f, ρ_m are the density of filler and medium, respectively. g is the acceleration due to gravity and d_f is the Stoke's diameter of the filler. η is the viscosity of the medium. K_{crowd} is the crowding factor that considers the increased concentration and can be related to the filler volume fraction, ϕ_f, through the following relation

$$K_{crowd} = (1 - \phi_f)^{4.5} \tag{3}$$

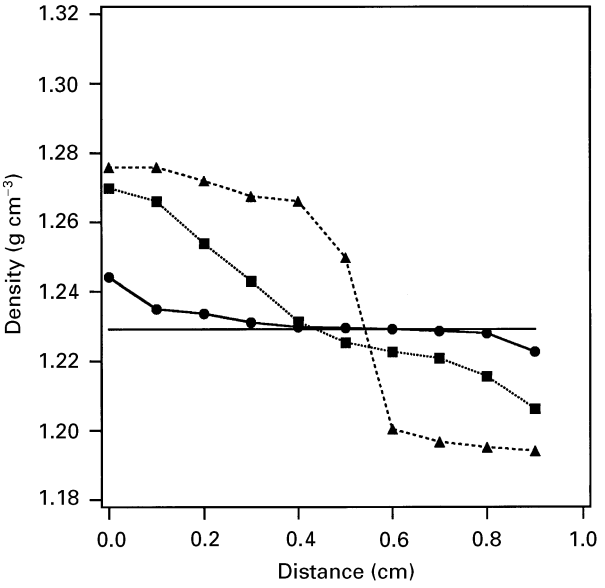

Figure 4 The density distribution of the functionally gradient epoxy/CF composite: rotation speed 1000 r.p.m., CF content 10 p.h.r., filler CF-M. Time: (—) 0 min, (●) 5 min, (■) 10 min, (▲) 20 min.

For our typical system, where ten parts of CF are mixed, the calculated volume fraction is 0.062. This implies that the motion of CF in this system will similarly follow Equations 2 and 3. In our system, the acceleration due to gravity, g, in Equation 2 should be replaced by 170 g which corresponds to the centrifugal effect of our centrifuging machine.

Fig. 4 shows the density distribution of the epoxy/CF composite with different rotation times. The end of the test tube, where the centrifugal force is the greatest, was set as zero distance. In this case, 10 p.h.r. CF (6.2% by volume) was included in the epoxy resin and the rotation speed was fixed at 1000 r.p.m. Rotation for 5 min did not much affect the density distribution and showed nearly the same density with the distance. Rotation for 10 min made the density distribution almost linear. But in the case of 20 min rotation, it was observed that CF and epoxy were clearly segregated from each other. Because no further movement of fibres may be allowed at the tube end, the fibres reaching the tube end become packed, resulting in a rapid increase of density. However, further packing of the fibres will not be permitted once the fibres are in the close-packed state. Therefore, the density in the region near the tube end increases slowly when the rotation time exceeds 10 min. In the region about 0.2 cm distance, fewer fibres were packed than in the region near the tube end, because many fibres moved towards the tube end. As a result, this region shows a slower increase of density. On the other hand, for the region beyond 0.5 cm, the density decreases with increasing rotation time. This fact indicates that in this region the distribution of fibres is achieved not by the packing of fibres but by the difference of velocities among the fibres with different lengths, which would

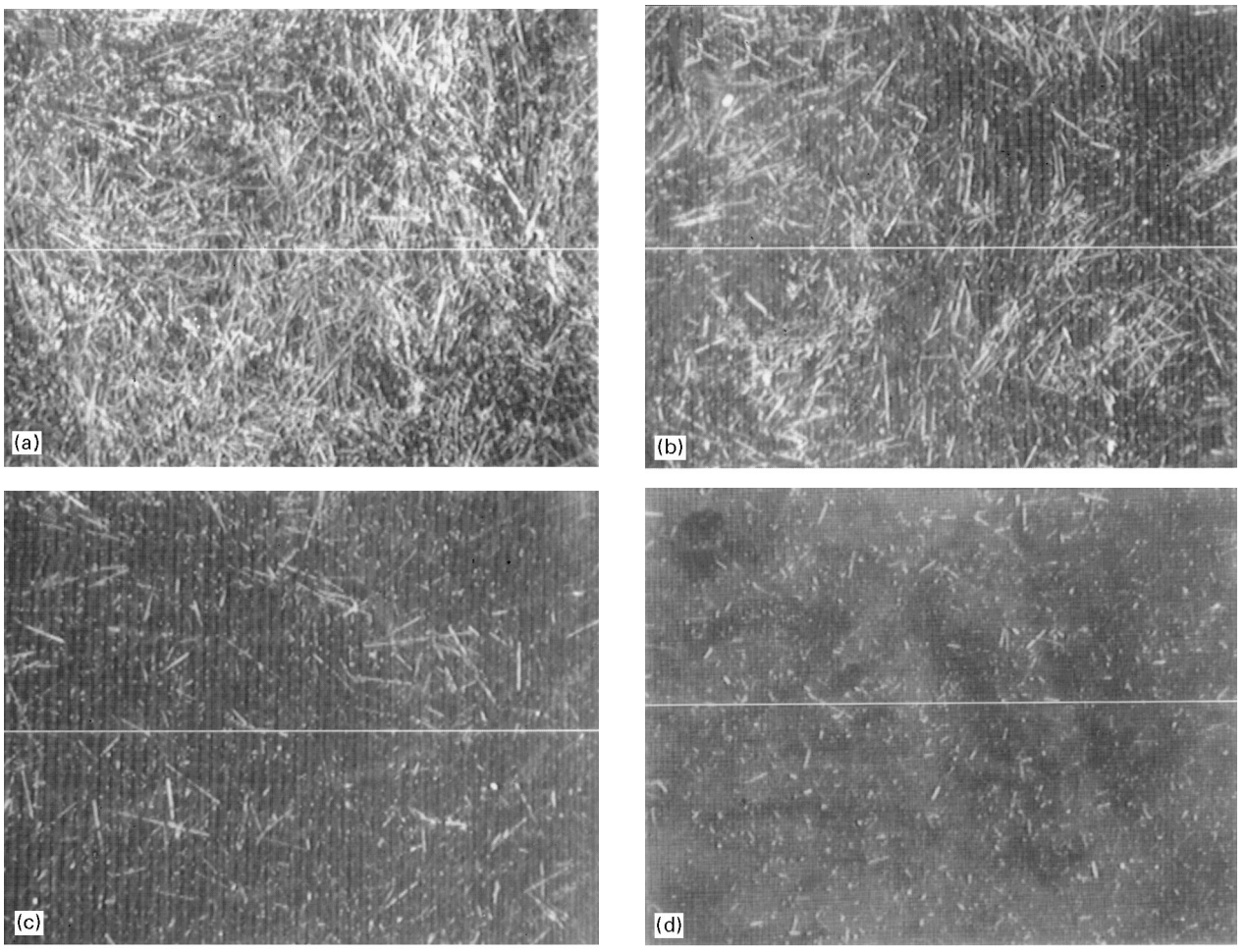

Figure 5 Micrographs of polished surfaces of the functionally gradient epoxy/CF composite: rotation speed 1000 r.p.m., rotation time 10 min, filler CF-M. (a) Distance 0 cm, (b) distance 0.25 cm, (c) distance 0.5 cm, (d) distance 0.75 cm.

be determined by Equation 2. Longer CFs moved at higher speed because they have higher mass than the shorter ones. The CFs used in this study had a broad length distribution. Therefore, once the centrifugal force is fixed, the settling velocities of CFs are different from one another.

Fig. 5 shows the videomicrographs of the cross-sections of the epoxy/CF composite along the distance from the bottom of the specimen. Fig. 5a shows that the bottom of the specimen has an agglomerated structure with many CFs. From considering the videomicrographs, the amount of CF is seen to have decreased as the distance increased.

3.1.2. Effect of the average length of the carbon fibre

Fig. 6 represents the density profiles for three samples in which 10 p.h.r. CF with different average fibre lengths were used. The epoxy/CF-S system exhibits the highest density near the end of the test tube and shows the largest density difference. However, its density profile is not linear. As the length of fibre increases and as the length distribution becomes broader, the system has more linear density distribution. The length or aspect ratio of the fibre is closely related to the maximum packing fraction corresponding to the randomly close-packed state [13, 14]. As the fibre length increases, more interstices or spaces would exist between the touching fibres, and hence lesser compaction of fibres ensues. This indicates that in the system

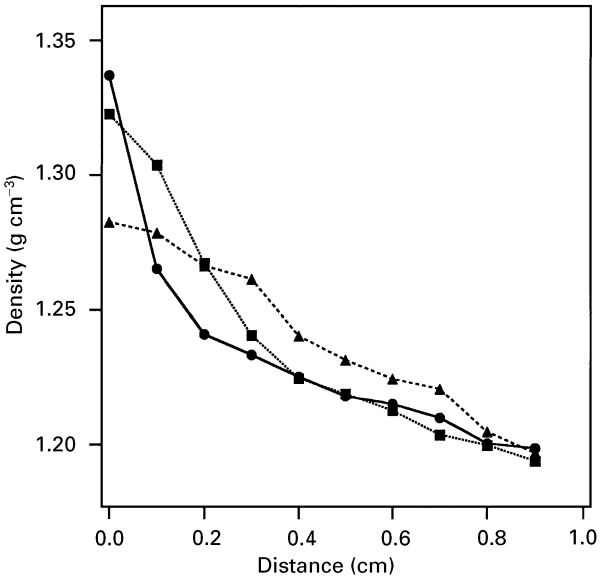

Figure 6 The density distribution of the functionally gradient epoxy/CF composite at different average lengths of CF: (●) CF-S, (■) CF-M, (▲) CF-L. Rotation speed 1000 r.p.m., rotation time 10 min.

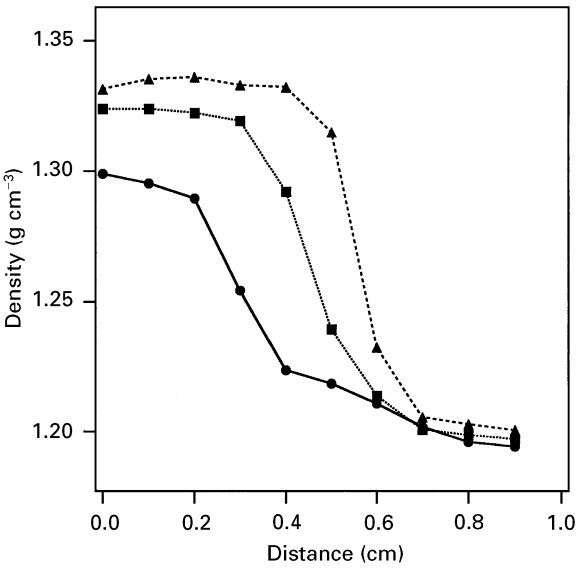

Figure 7 The density distribution of the functionally gradient epoxy/CF composite at different CF contents: (●) 10 p.h.r., (■) 15.4 p.h.r., (▲) 21.2 p.h.r. Rotation speed 1000 r.p.m., rotation time 10 min, filler CF-M.

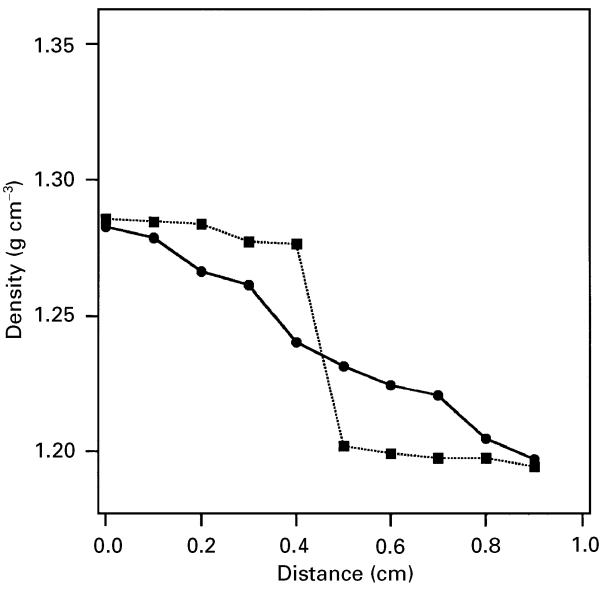

Figure 8 The density distribution of the functionally gradient epoxy/CF composite at different temperatures: (●) 28 °C, (■) 18 °C. Rotation speed 1000 r.p.m., rotation time 10 min, filler CF-L.

using longer fibres with a broader distribution, it is easier to have a more linear density profile for a given set of experimental conditions.

3.1.3. Effect of the content of carbon fibre

Fig. 7 shows the effect of the content of CF on the density distribution of the epoxy/CF composite. When 15.4 p.h.r. CF were contained, the volume per cent of CF in the epoxy matrix was 1.5 times as large as that of 10 p.h.r. In the case of 21.2 p.h.r., the volume per cent of CF was twice as large as that of 10 p.h.r. As the content of CFs increased, the ratio of the length of the fibre-packed region to the total specimen length tended to increase, and the density difference between the bottom and the upper region of the specimen became larger. The density of the bottom region in the case of high CF content was higher than that in the case of low CF content. This phenomenon is explained as follows. At a low fibre content, the movement of fibres due to the applied force is governed by Stoke's law or its modified version, such as Equation 2. For this system, the individual fibres are relatively free to move, regardless of other fibres, in such a way that longer fibres, which have larger Stoke's equivalent diameter, move with a higher velocity than shorter ones. Hence, longer fibres would first reach and be packed at the tube end. However, as the volume fraction of fibre increases, the fibre–fibre interactions make it difficult for individual fibres to move with velocities depending only on the Stoke's equivalent diameter. Instead, a cooperative motion of long and short fibres is likely to occur, which increases the packing efficiency of the fibre-packed region. This enhancement in packing efficiency is thought to induce the higher density of the system with higher fibre content near the tube end.

3.1.4. Effect of resin viscosity

Fig. 8 shows the effect of temperature that is closely related to the system viscosity on the density gradient profiles. When the temperature is high, a step-like density profile is formed for a given rotation time. In this case, the terminal velocity of all fibres is so high that the difference of velocities between moving fibres makes only a minor contribution to the density gradient formation. On the other hand, when the temperature is low, the obtained density profile is almost linear. Reduced velocities and packing rate of fibres near the tube end, together with the gradient formation due to the velocity difference of fibres, account for this linear density distribution.

3.2. Orientation of carbon fibres

Because CFs are geometrically anisotropic, they are subject to preferential orientation during moving and packing, through the action of centrifugal force. This fact results in anisotropy in properties such as mechanical and electrical properties.

Fig. 9 represents the volume resistivities of the thin sections of the epoxy/CF composite. The resistance was measured parallel to the direction of the centrifugal force. The conductivity of the composite composed of conductive filler depends on the content of fillers, geometric shape, and the interaction between filler and matrix. According to the percolation theory, the percolation threshold, i.e. minimum concentration in which the conductive fillers are structured to conduct the electricity, decreases abruptly when the fillers are long and well oriented [15–17]. Generally, in the case where the fibres are aligned in one direction, the resistivity in the direction perpendicular to the orientation is one-tenth of that in the parallel direction [18]. This means that the measured resistivity reflects not only the content of fibres present, but also their orientation

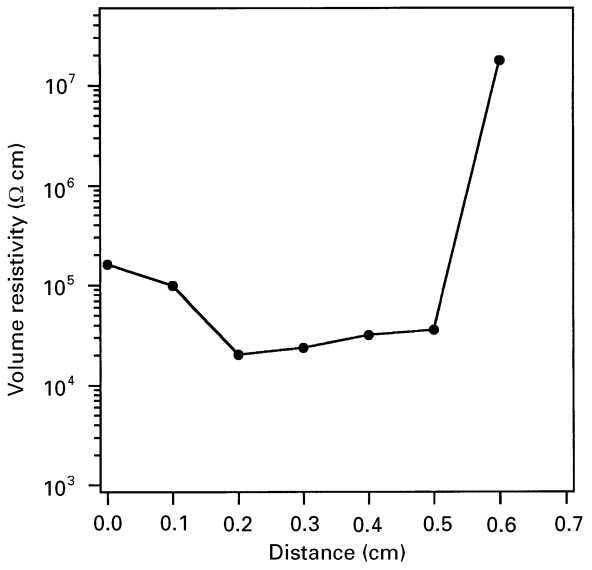

Figure 9 Volume resistivity distribution of a composite prepared with gold-coated CF as a function of distance: rotation speed 1000 r.p.m, rotation time 10 min.

with respect to the measuring direction. In the region above 3 mm from the bottom of the specimen, the resistivity increases with the distance from the bottom of the specimen, because this region has more epoxy whose volume resistivity is high. However, below 3 mm, the resistivity increases despite the increase of CF content (as the distance decreases). The above result suggests that CFs are aligned perpendicular to the direction of centrifugal force as the CFs are packed at the bottom of the test tube. A similar result was also observed in the optical microscopy analysis.

3.3. The mechanism of formation of the gradient structure

3.3.1. Packing mechanism

When centrifugal force is applied to the isotropic dispersion of fibrous fillers, the fillers move along the direction of the centrifugal force. However, at the bottom of the test tube, the fillers are prevented from moving and are packed. The fillers packed initially are condensed by the centrifugal force and the pressure of the fillers in the upper region of the test tube. These phenomena make the bottom region of the specimen denser than the upper region. It was observed that this packing mechanism occurred mainly at the bottom of the specimen.

3.3.2. Settling mechanism

When constant centrifugal force was applied, the fillers settled at different speeds because of the different masses of fillers. Long fibres settled faster than shorter ones. As a consequence, the bottom region was rich in long fibres and the upper region was rich in short fibres. This settling mechanism occurred mainly in the upper and middle regions of the specimen.

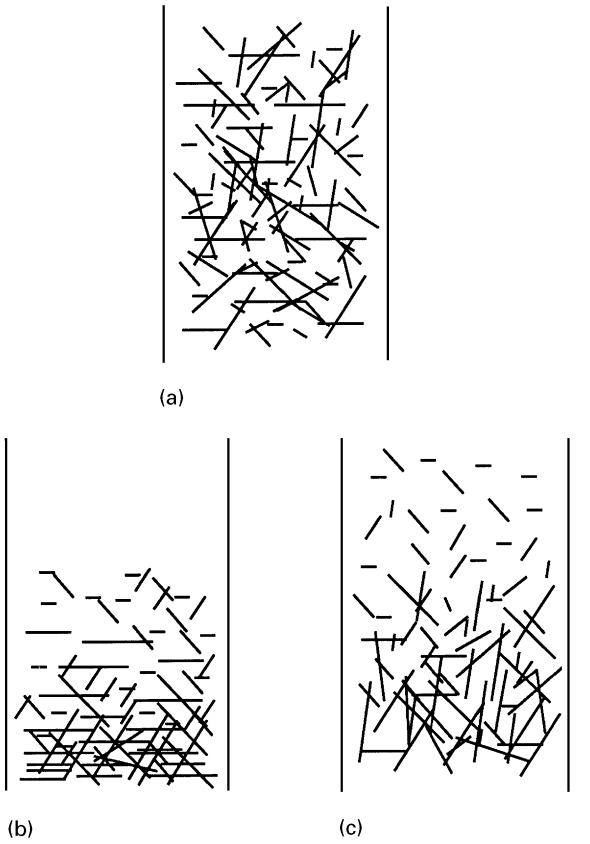

Figure 10 Schematic illustration of the mechanism of compositional gradient formation: (a) the isotropic state, (b) the packing mechanism, (c) the settling mechanism.

3.3.3. Formation of gradient structure

Fig. 10 represents the schematic diagram of two mechanisms explained above. When centrifugal force is applied to an isotropic state of the CFs and epoxy mixture (Fig. 10a), CFs are packed to form a gradient structure in the bottom region of the specimen (Fig. 10b), and in the upper region, CFs are settled at different speeds to form a gradient structure (Fig. 10c).

3.4. The flexural property of the functionally gradient composite

To investigate the characteristics of the flexural property of the functionally gradient composite, a bar-shaped specimen was prepared under the conditions given in Table II. The case in which the specimen was loaded at the fibre-rich surface (Fig. 11a, Type A) and the case in which the specimen was loaded at the fibre-rare surface (Fig. 11b, Type B) were compared with each other.

Table III shows the flexural properties of each specimen, including those of isotropic composite and pure epoxy. In the case of flexural modulus, known to be relatively insensitive to microstructure, three epoxy/CF composites had similar values and showed 50% improvement over the pure epoxy. The flexural strength of type A was higher than that of the isotropic composite, but type B exhibited a lower value.

Fig. 12 shows a typical load–displacement curve of the flexural test. Pure epoxy (Fig. 12a) shows a low

TABLE II Preparation conditions of the functionally gradient epoxy/CF composite for the flexural test

Condition	Remark
CF content	10 p.h.r. (6.2 vol %)
Average length of CF	160 μm
Rotation speed	1000 r.p.m.
Rotation time	10 min

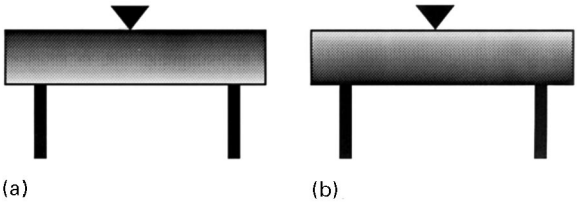

Figure 11 Flexural test of the functionally gradient epoxy/CF composite.

TABLE III Flexural properties of the epoxy/CF composites

	Flexural strength (MPa)	Flexural modulus (GPa)	Yield strain (%)
Epoxy	122.7	2.02	0.085
Isotropic	118.3	3.01	0.044
[a]	130.0	2.83	0.055
[b]	87.5	2.94	0.031

[a]Loaded at the fibre-rich surface.
[b]Loaded at the fibre-rare surface.

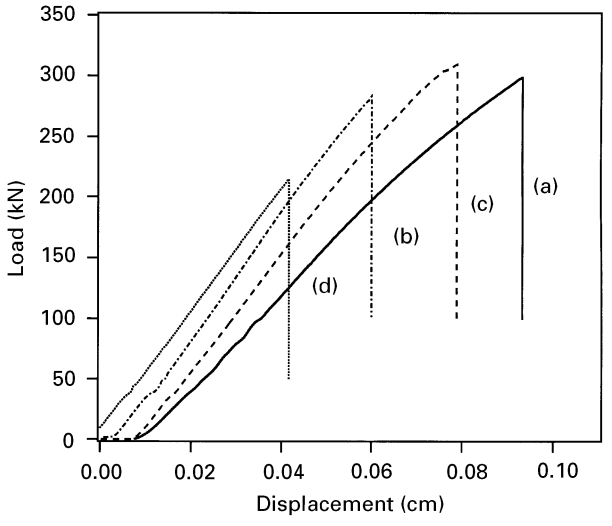

Figure 12 Typical load–displacement curve of the flexural test: (a) neat epoxy, (b) isotropic composite (10 p.h.r.), (c) loaded at the CF-rich surface, (d) loaded at the CF-rare surface, (c, d) the functionally gradient composite (1000 r.p.m., 10 min).

slope, large elongation and deviation from the linear slope before fracture. The isotropic composite (Fig. 12b) shows a high, linear slope and short elongation. The load–displacement curve of type A (Fig. 12c) showed the deviation from the linearity before fracture, as did pure epoxy. However, type B (Fig. 12d) showed linearity before fracture, as in the isotropic composite. This result indicates that the mechanical property of the bottom area of the specimen, which undergoes tensile stress, makes a major contribution to the flexural strength of the epoxy/CF composite. In type A, the absence of CF in the side opposite to the loading direction would result in more elongation, and a greater abundance of CF at the loading side would give rise to greater resistance to the compressive force. These two effects, originating from the unique internal structure, are thought to be responsible for the higher flexural strength. To explain the above result, the tensile and compression tests of isotropic epoxy/CF composite with various CF contents were carried out.

Tensile and compressive properties of the epoxy/CF composites are depicted in Figs 13 and 14. As the content of CF increased, tensile strength and tensile modulus increased. In particular, the tensile strain at break decreased as the content of CF increased. Compressive strength also increased, but a lower degree of increment was observed than in the case of tensile strength. The compressive property was not greatly affected by CF content, but the tensile strain at break decreased with increasing CF content. These results could explain the higher flexural strength of the Type A specimen.

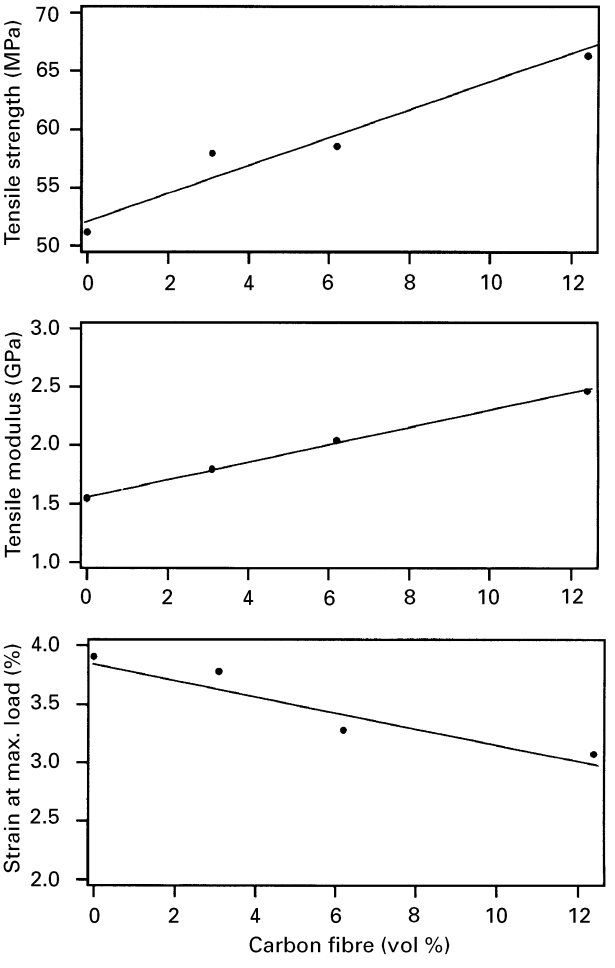

Figure 13 Tensile properties of epoxy/CF composite as a function of CF content.

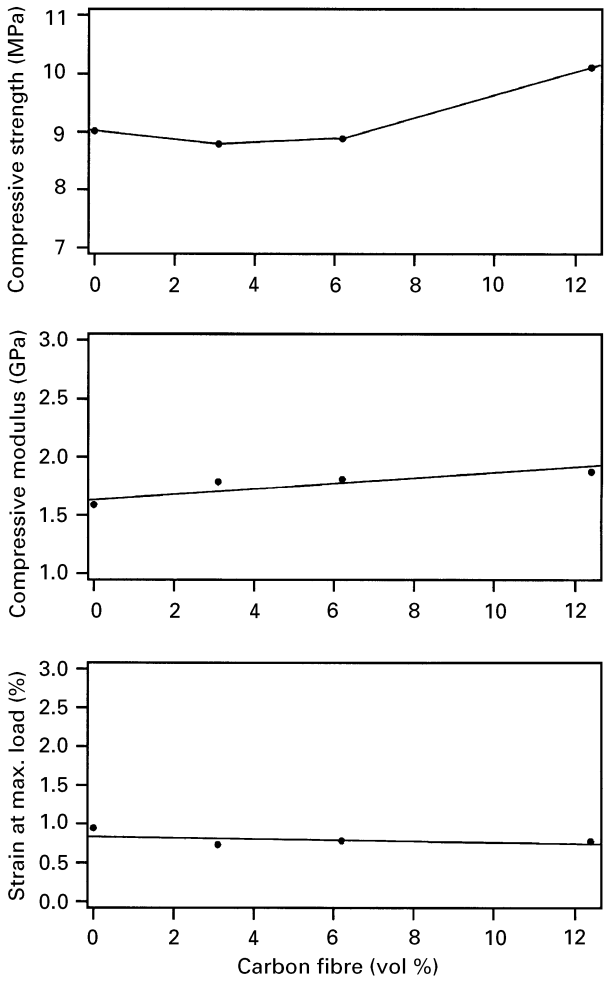

Figure 14 Compressive properties of epoxy/CF composite as a function of CF content.

4. Conclusions

1. The functionally gradient epoxy/CF polymeric composite could be effectively manufactured using centrifugal force.

2. A gradient structure was formed by the packing of CFs in the bottom region of the specimen and the settling of CFs in the upper region. The gradient structure was controlled by variation of the rotation time, average fibre length, resin viscosity and fibre content.

3. At the bottom of the specimen, CFs were aligned perpendicular to the direction of centrifugal force. However, in the upper region, CFs were aligned parallel to the direction of centrifugal force.

4. When a flexural load is applied to the surface with a high CF content, the flexural strength of the functionally gradient epoxy/CF composite was higher than that of the isotropic one, due to its unique internal structure.

References

1. M. NIINO and S. MAEDA, *Kinou Zairyo*, **10** January (1990) 22.
2. *Idem*, *ISIJ Int.* **30** (1990) 699.
3. H. OKAMURA, *Mater. Sci. Eng.* **A143** (1991) 3.
4. T. KITANO, Private communication (1993).
5. Y. FUKUI, H. KINOSHITA, and K. NAKANISHI, *JSME Int. J. Ser. I* **35** (1992) 95.
6. Y. TSUNEKAWA, M. OKUMIYA, I. NIIMI and K. YONEYAMA, *J. Mater. Sci. Lett.* **7** (1988) 830–832.
7. T. NISHIDE *et al.*, in "Handbook of New Materials" (1993). The Polymer Society of Japan, p. 618 (in Japanese).
8. L. M. SHEPPARD, *Ceram. Bull.* **71** (1992) 617.
9. M. NIINO, Private communication (1988).
10. Y. MIYAMOTO, *Kogyo Zairyo* **39** (1991) 58.
11. M. FUNABASHI, E. AOKI, Y. NAGATSUKA and K. KITANO, in "Proceedings of the 2nd Japan International SAMPE Symposium", 11–14 December (1991) pp. 663–70.
12. R. D. NELSON Jr, in "Handbook of Powder Technology, Vol 7. Dispersing Powders in Liquids". J. C. Williams and T. Allen (eds), (Elsevier, Amsterdam, 1988) Ch. 8.
13. J. V. MILEWSKI and H. S. KATZ, in "Handbook of Reinforcements for Plastics". J. V. Milewski and H. S. Katz (eds), (Van Nostrand Reinhold, New York, 1987) Ch. 13.
14. J. V. MILEWSKI, in "Additives for Plastics" (New Developments, Academic Press, New York, 1980). R. B. Seymour (ed), p. 5.
15. V. K. S. SHANTE and S. KIRKPATRICK, *Adv. Phys.* **20** (1971) 325.
16. M. BLASZHIEWICZ, D. S. McLACHILAN and R. E. NEWNHAM, *Polym. Eng. Sci.* **32** (1992) 421.
17. P. J. GANS, *J. Chem. Phys.* **42** (1965) 4195.
18. R. A. CROSSMAN, *Polym. Eng. Sci.* **25** (1985) 507.

Received 16 February
and accepted 17 September 1996